Iraqi Journal for Computer Science and Mathematics

Manuscript 1282

Diagnosis of COVID-19 and Viral Pneumonia with Chest X-Ray Images Using ResNet-34

Sudhir Anakal

Krishna Prasad K

Chandrashekhar Uppin

Dileep Kumar M

IRAQI JOURNAL FOR COMPUTER SCIENCE AND MATHEMATICS 2025;6:160–170

ORIGINAL STUDY

Diagnosis of COVID-19 and Viral Pneumonia with Chest X-Ray Images Using ResNet-34

Sudhir Anakal [a,b,*], **Krishna Prasad K** [c], **Chandrashekhar Uppin** [d], **Dileep Kumar M** [e,f]

[a] Institute of Computer Science and Information Science, Srinivas University, Mangalore, Karnataka, India
[b] Faculty of Computer Applications, Sharnbasva University, Kalaburagi
[c] Department of Cyber Security & Cyber Forensics, Srinivas University, Mangalore, Karnataka, India
[d] Faculty of Science & Computing, Hensard University,Nigeria
[e] Hensard University, Nigeria
[f] International Research Fellow - SEGi University, Malaysia

ABSTRACT

COVID-19 is a highly contagious viral infection that primarily affects the respiratory system, causing symptoms such as high fever, cough, and severe respiratory distress. Early detection of the disease is of utmost importance to control the spread and severity. Common diagnostic methods include Reverse Transcription Polymerase Chain Reaction (RT-PCR), antigen tests, chest X-rays, and computed tomography (CT) scans. Similarly, viral pneumonia, another severe lung infection, leads to fluid or pus accumulation in the lungs, causing symptoms such as chest pain, fatigue, excessive sweating, and nausea. The elderly and young children are particularly vulnerable to severe complications. Similarly, viral pneumonia, another severe lung infection, leads to fluid or pus accumulation in the lungs, causing symptoms such as chest pain, fatigue, excessive sweating, and nausea. The elderly and young children are particularly vulnerable to severe complications. This paper aims to get the bottom of the ResNet-34 model, for detecting COVID-19 and Viral Pneumonia using radiography images and to build a web application using a Streamlit framework for detecting the presence of the disease. The ResNet-34 is a Convolutional Neural Network (CNN) model used to classify COVID-19, Viral Pneumonia, and normal (negative) among 15000 Chest X-ray images. In this work, datasets from Kaggle repository have considered that help to acquire Chest X-ray images as these are extensively used to diagnose COVID-19 and Viral Pneumonia as they give clear insights into the lungs. The presented resNet-34 model, helps to discriminate between COVID-19 and Viral Pneumonia with high accuracy and precision.

Keywords: COVID-19, Viral Pneumonia, ResNet-34, PyTorch, Chest X-ray images, Streamlit

1. Introduction

The outbreak of COVID-19, caused by the Severe Acute Respiratory Syndrome Coronavirus 2 (SARS-CoV-2), has posed a significant global health challenge, leading to widespread morbidity and mortality [1, 2]. Early and accurate diagnosis of COVID-19 is crucial for timely medical intervention and containment of the virus. The standard diagnostic method, Reverse Transcription Polymerase Chain Reaction (RT-PCR), is widely used; however, it has limitations such as long processing times and a relatively high false-negative rate [3]. Medical imaging techniques such as chest X-rays (CXR) and computed tomography (CT) scans have emerged as valuable complementary tools for COVID-19 detection, offering rapid and non-invasive screening capabilities [4–6].

Viral pneumonia, another respiratory infection, shares many symptomatic and radiographic characteristics with COVID-19, making accurate

Received 26 December 2024; revised 22 May 2025; accepted 22 May 2025.
Available online 4 July 2025

* Corresponding author.
E-mail addresses: sudhir.anakal@gmail.com (S. Anakal), krishnaprasadkcci@srinivasuniversity.edu.in (Krishna Prasad K), cvuppin@gmail.com (C. Uppin), prof.dr.dil@gmail.com (Dileep Kumar M).

https://doi.org/10.52866/2788-7421.1282

differentiation essential for appropriate treatment (Kanne, 2020). Both conditions lead to lung opacities and inflammation, complicating visual diagnosis by radiologists. A vital tool for identifying and tracking respiratory disorders is medical imaging, such as CT scans and chest X-rays [16–18]. Early intervention is made possible by radiographic imaging, which offers instant insights into lung diseases in contrast to time-consuming techniques like RT-PCR. Automated image analysis can further improve diagnostic speed and accuracy by utilizing developments in deep learning and machine learning [19–21]. Deep learning-based techniques, particularly Convolutional Neural Networks (CNNs), have demonstrated remarkable potential in automating the classification of medical images with high accuracy and reliability. Among CNN architectures, the Residual Neural Network (ResNet) family, particularly ResNet-34, has shown efficiency in medical image analysis by addressing the vanishing gradient problem and enhancing feature extraction. Chest X-ray (CXR) is a valuable diagnostic tool for COVID-19 and pneumonia detection. Deep learning architectures like ResNet, Inception, and Googlenet have been employed to differentiate COVID-19 pneumonia from other types, though challenges in accurate diagnosis persist [23–26].

To classify chest X-ray pictures into three categories—Normal, COVID-19, and Viral Pneumonia—this study investigates the creation of a diagnostic model using ResNet-34. In early tests, ResNet-34 outperformed more straightforward designs like ResNet-18 and CheXNet, providing a strong framework for feature extraction and classification. By offering dependable, quick, and understandable data, the model seeks to support healthcare providers by cutting down on diagnostic turnaround times and possibly enhancing patient outcomes. Using the Streamlit framework, the model has been implemented as a web application to guarantee wider applicability. This enables healthcare providers to submit X-ray pictures and obtain real-time predictions. This research fills important gaps in diagnostic efficiency, especially in situations with low resources, by fusing state-of-the-art deep learning algorithms with easily accessible technology.

2. Literature review

Hussain et. al. [5] has developed a model using CoroDet which is a CNN model for COVID-19 detection. In his research, he has taken some of the COVID-19 and Normal CT scans and Chest X-ray images for identification of the disease. In this paper, they have claimed that this model is capable of detecting COVID-19 and Normal classes with 97% accuracy, Pneumonia (Non-COVID) with 94% and the inclusion of bacterial Pneumonia (non-COVID) with 91%. Nayak et. al. [6] has come up with 8 pre-trained CNN models, which include Inception-v3, AlexNet, VGG16, SqueezeNet, ResNet34 and 50, GoogleNet and MobileNet for diagnosis of COVID-19 with the Chest X-ray images of normal lungs. In this paper, they have analyzed all eight CNN models and have taken only those models that have made up to their expectations by considering some of the vital hyper-parameters of the model.

Wang et. al. [7] ventured into the study of building a model with the sophisticated algorithms available in deep learning. They introduced COVIDNet, a CNN model for COVID-19 Detection from the radiography Chest X-ray images. In this paper, they emphasized that the COVIDNet is the first such CNN model for detecting COVID-19 with Chest X-ray images at the time of its release. Sekeroglu et. al. [8] has published a paper on the detection of COVID-19 using radiography images. In his research he has taken 5 machine learning algorithms for training the datasets, several trials were carried out on CNN models and tried out using transfer learning. They have utilized publicly available Chest X-ray images for COVID-19, Pneumonia and Normal classification, and have achieved sensitivity mean, specificity mean and accuracy of 93%, 99%, and 98% respectively. Rajpurkar et. al. [9] has published their research in Pneumonia detection with the help of Chest X-ray images. In this paper, he has built a CheXNet, a CNN model that helps in detecting not only Pneumonia, but also other lungs related 14 diseases. The CheXNet is 121 layers deep and takes radiography images as input predicts the disease with 85% accuracy and even highlights the portion of the lungs where it is exposed to pneumonia. Kochgaven et. al. [10] Published a study for detecting the presence of COVID-19 using the ResNet-18 model. The ResNet-18 is a CNN model which comes up with 18 layers and this model was deployed using the transfer learning technique. In this research, they have obtained an accuracy of 97% and a sensitivity rate of 96%. We have taken up this work and have implemented the Chest X-ray images with a different model i.e., ResNet-34, which comes with 34 layers and have observed how the model would work with a more layered pre-trained model.

The study as presented in [20] evaluates seven machine learning algorithms for early cardiovascular disease detection, finding that the multilayer perception achieved over 88% accuracy, while the decision tree performed the poorest with over 79% accuracy, highlighting the effectiveness of these techniques.

Deep learning models, specifically ResNet50 and EfficientNet-B0, analyze chest X-ray images to diagnose COVID-19 and viral pneumonia. EfficientNet-B0 achieved a higher accuracy of 93.08%, aiding in accurate differentiation and timely medical interventions for effective patient management [23]. In this work, the authors have implemented Contrast Limited Adaptive Histogram Equalization (CLAHE) for image preprocessing by using deep learning models, such as ResNet50 and EfficientNet-B0 for prediction.

In [24], the authors have proposed 42-layer CNN model in the study effectively diagnoses COVID-19 and distinguishes it from NORMAL and PNEUMONIA_VIRAL cases using chest radiology imaging techniques, outperforming previous models in accuracy and complexity of detection scenarios.

3. Problem statement

In the medical field, accurately and promptly diagnosing respiratory conditions, such as COVID-19 and viral pneumonia, is still a major difficulty. Conventional diagnostic techniques like RT-PCR and antigen testing are frequently laborious and logistically challenging, especially in environments with limited resources. These drawbacks have brought attention to the necessity of alternate diagnostic techniques that can yield accurate and timely results. As a quicker and easier diagnostic approach, chest X-ray imaging has become a competitive alternative for identifying respiratory disorders. Nevertheless, manual X-ray image interpretation is subject to error and necessitates a high level of skill, which not all medical institutions may have on hand. This variation frequently leads to erroneous or delayed diagnoses, which could jeopardize patient outcomes.

A promising solution is provided by machine learning and deep learning algorithms, which automate the analysis of chest X-ray pictures. The effectiveness of these techniques has been shown in much research, however, problems including dataset biases, poor model interpretability, and generalization to various clinical contexts still exist. Current models frequently fall short of addressing these problems in their entirety, which restricts their usefulness in actual situations. By utilizing ResNet-34 to create a reliable diagnostic model for dividing chest X-ray pictures into three groups—Normal, COVID-19, and Viral Pneumonia—this study seeks to close these gaps. To improve automated X-ray image analysis's accuracy, dependability, and clinical relevance, this study makes use of transfer learning, sophisticated preprocessing methods, and interpretability tools like Grad-CAM. Additionally, even in contexts with limited resources, accessibility and usability are guaranteed by the model's distribution as a web application.

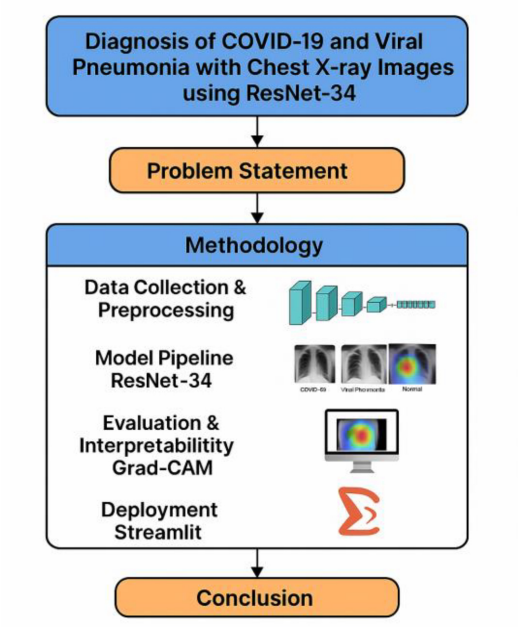

Fig. 1. Graphical representation of proposed work frame.

4. Methodology

This study follows a structured deep learning approach to develop and evaluate a diagnostic model for detecting COVID-19 and viral pneumonia from chest X-ray images. A graphical representation of the proposed work frame is shown in Fig. 1. The following are the steps (1–6) for the proposed study.

- *Step 1: Data collection and preprocessing.*

  A dataset comprising 15,153 chest X-ray images was obtained from the Kaggle repository. The dataset is categorized into three classes: Viral Pneumonia (1,345), COVID-19 (3,616), and Normal (10,192), as detailed in Table 1. Fig. 2 shows the images of (a) COVID-19, (b) Normal , (c) Viral Pneumonia.

  To mitigate class imbalance, data augmentation techniques such as random rotations, flipping, and scaling are applied. Additionally, oversampling is used to ensure fair representation of minority

Table 1. Images used for training and testing of the model.

Class	Number of Training Images	Number of Testing Images
COVID-19	3616	3616
Normal	10,192	10,192
Viral Pneumonia	1345	1345

Fig. 2. Images of (a) COVID-19, (b) Normal (b), (c) Viral Pneumonia.

classes. All images are resized to 224 × 224 pixels to match ResNet-34's input requirements, and pixel values are normalized for stable training.

- *Step 2: Model architecture.*
  The ResNet-34 architecture is selected due to its deep residual learning capabilities, which enhance gradient flow and mitigate the vanishing gradient problem. Transfer learning is applied by initializing the model with pre-trained ImageNet weights, followed by fine-tuning layers to better capture medical imaging features.
- *Step 3: Training and validation strategy.*
  The dataset is split into training (70%), validation (15%), and testing (15%) subsets using stratified sampling to maintain class balance. Model training is conducted using:
  - Loss function: Cross-entropy
  - Optimizer: Adam
  - Regularization: Early stopping based on validation loss to prevent overfitting
  - Validation: Five-fold cross-validation for robust performance assessment
- *Step 4: Performance metrics.*

The model is evaluated using multiple classification metrics to ensure reliability:

a) Accuracy: Overall classification correctness
b) Precision & Recall: Measures of specificity and sensitivity
c) F1-score: Harmonic mean of precision and recall
d) AUC-ROC: Discriminative ability between classes
e) Confusion Matrices: Analysis of classification patterns
f) *Misclassification Analysis and Interpretability*

Misclassified images are examined to identify trends and potential areas for model improvement. Grad-CAM (Gradient-weighted Class Activation Mapping) is employed to generate heatmaps, highlighting critical regions in X-ray images that influenced model predictions. This enhances model explainability in medical AI applications.

- *Step 5: Web-based deployment.*
  The trained model is deployed as a web application using Streamlit, providing an interactive platform for uploading chest X-ray images and obtaining real-time predictions. The application also displays Grad-CAM heatmaps alongside probability scores for each class, improving interpretability.
- *Step 6: Usability testing and clinical validation.*
  To enhance practical applicability, usability testing is conducted with input from medical professionals, refining the interface and ensuring ease of use in clinical settings.

For developing the model, we have imported some of the libraries which include Torch, Torch is the main library that is used to build, train, and test the ResNet-34 model. Torchvision, this library is used to transform the images into 224*224 pixels, because the ResNet-34 is recommended to take 224*224-pixel images. Along with them, we have also used the Matplotlib library for displaying the images and depicting plots for showing the validation and training losses. CNN is typically used for object detection, image classification, speech recognition and some other applications [6]. The ResNet-34 model is used to steer clear of the degradation problem faced by some other CNN models i.e., when developers started to add more layers to their CNN model to get more accuracy, they encountered one problem that is at a certain point the model's accuracy started to saturate. Then ResNet-34 model came to rescue developers from this issue, with its many layers it is very easy to train the model with very less training errors. Fig. 3 shows ResNet-34 architecture.

CNN model has three layers naming convolutional layer, a pooling layer followed by fully connected

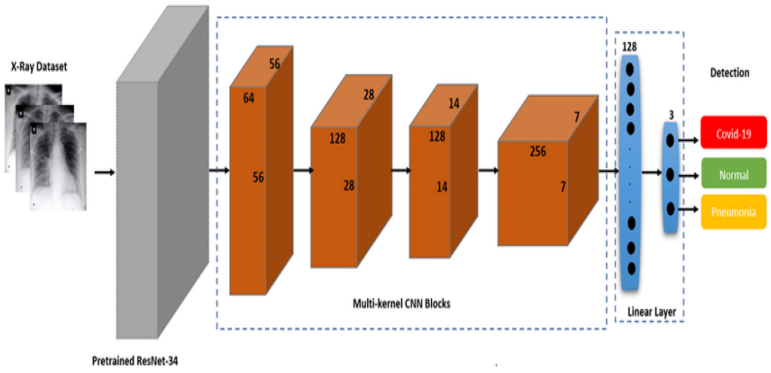

Fig. 3. ResNet-34 architecture.

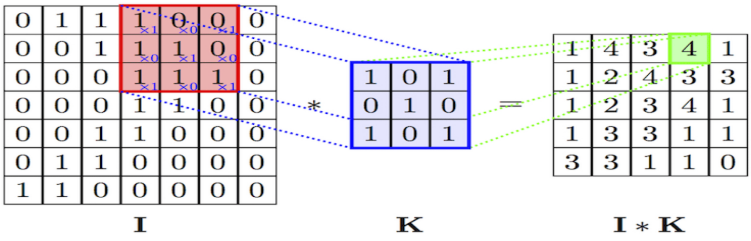

Fig. 4. Working structure of the convolution operation.

layers. The convolution layer is the first layer of the ResNet model, because of this layer CNN is named a Convolutional Neural Network [6]. As shown in Fig. 1 we have taken 3*224*224 as the input image, which means that we are initializing 3 filters with 224*224-pixel image and taking stride 1 (moving one step after another in the convolution). This input image is then sent to perform the convolution operation in which 3*3 filters are used upon the input image to get the dot product i.e., each value in the filter is multiplied with each pixel in the input image and an addition operation is performed over those values to get the feature map. Consider Fig. 4 to get a better understanding of convolution operation.

Once the feature map is out then it is passed through the batch normalization phase to speed up of training process and to increase the learning rate so that the model can learn more easily and rapidly. After batch normalization, the feature map is sent to the pooling layer, before it is sent to the pooling layer an activation function is applied to the feature map to pull out all the negative values from it. In this model, we are using the Rectified Linear Unit (Relu) activation function to perform this task. This activation function is used most often in the CNN models. The formula to perform the activation function is, $y = \max(0, x)$. Relu function replaces all negative values in the feature map with zero (0) and leaves positive values intact. Then the feature map is taken to the pooling layer where we extract the most unique features of the image. There are two types of pooling max pooling and average pooling as shown in Fig. 5.

In the case of max pooling, we are going to take a maximum number out from the feature map i.e., these numbers are allocated based on the unique (from which we can easily predict the given image) feature of the image. And in the average pooling, we will sum up the 4 numbers from each block and make an average of it. For example, in Fig. 5 we are adding $(2+3+4+7)$ and dividing it by 4 then we get the final value as 4 which will be updated in the 2D feature map. The 2*2 matrix of the pooling layer is flattened before we get into the fully connected layer. Flattening is a process of converting the 2d feature map into a one-dimensional array [9]. This conversion is of utmost importance because we cannot feed the 2d image to the fully connected neurons so firstly we need to convert them into the one-dimensional array and update these values in each neuron as shown in Fig. 6.

With the advent of a fully connected layer model training takes place. We need to set some of the hyperparameters of the ResNet-34 model which includes the batch size, learning rate, shuffle, and so on. In this model, we have taken batch size as 6 and a learning rate of 3e-5 (0.00003). The reason for taking the batch size is to minimize the system requirements for training the model. If we give a complete dataset for training of the model, then it requires high computational resources such as RAM and GPU.

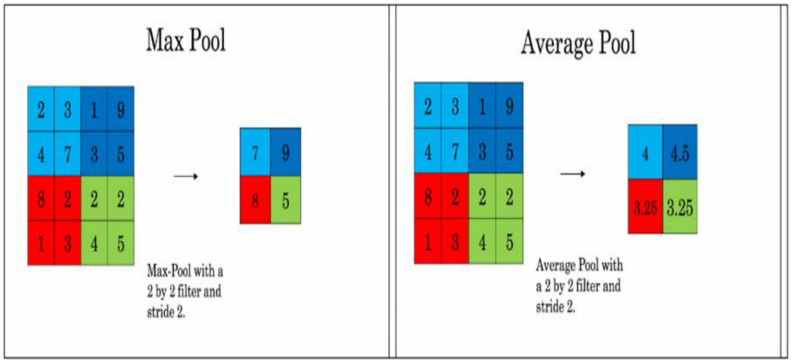

Fig. 5. Pooling layer.

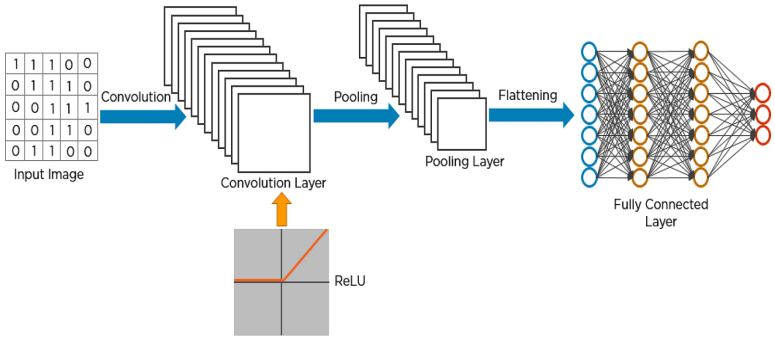

Fig. 6. Feature extraction process.

We are training our model for one epoch i.e., one epoch contains several iterations. For example, our dataset contains a total of 15,153 samples of all three classes, now this number is divided by the batch size, viz 15,153/6 then we will have 2526 as the output value. The output value is the number of iterations in one epoch. 6 samples from 3 classes go for one forward propagation and one backward propagation to complete one iteration. These samples flow from initial neurons through the hidden layer to the output layer, in between each neuron updates its weights along with the bias and an activation function Relu is used to fire the neuron [8]. The model arrives at the output layer with the predicted value and this predicted value is compared with the actual value, if you find a change then we are going to update the predicted value with the actual value using the loss function. The loss/cost function is defined using (actual value – predicted value) ˆ2. In this context, the loss would be more as the model predicted incorrectly; to reduce the loss we need to use the optimizers. Adam's optimizer is used in this model. Then starts the back-propagation, in this process, the model updates all the weights according to the value which we have updated using the loss function. This procedure continues until we get a reliable accuracy with a relative reduction in the loss. Fig. 7 depicts validation and training loss after the completion of the training process.

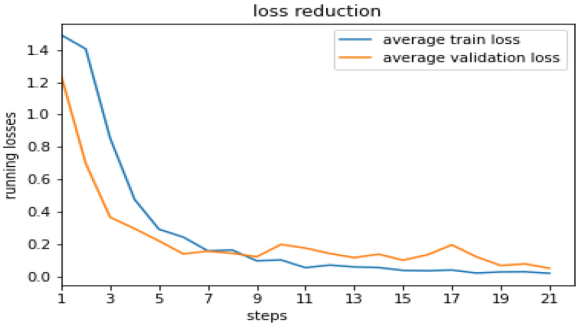

Fig. 7. Average training and validation loss.

With the advent of a fully connected layer model training takes place. We need to set some of the hyperparameters of the ResNet-34 model which includes the batch size, learning rate, shuffle, and so on. In this model, we have taken batch size as 6 and a learning rate of 3e-5 (0.00003). The reason for taking the batch size is to minimize the system requirements for training the model. If we give a complete dataset for training of the model, then it requires high computational resources such as RAM and GPU. We are training our model for one epoch i.e., one epoch contains several iterations. For example, our dataset contains a total of 15,153 samples of all three classes, now this number is divided by the batch size, viz 15,153/6 then we will have 2526

as the output value. This output value is the number of iterations in one epoch. 6 samples from 3 classes go for one forward propagation and one backward propagation to complete one iteration. These samples flow from initial neurons through the hidden layer to the output layer, in between each neuron updates its weights along with the bias and an activation function Relu is used to fire the neuron [8–10]. The model arrives at the output layer with the predicted value and this predicted value is compared with the actual value, if you find a change then we are going to update the predicted value with the actual value using the loss function. The loss/cost function is defined using (actual value – predicted value) ˆ2. In this context, the loss would be more as the model predicted incorrectly; to reduce the loss we need to use the optimizers. Adam's optimizer is used in this model. Then starts the backpropagation, in this process, the model updates all the weights according to the value which we have updated using the loss function. This procedure continues until we get a reliable accuracy with a relative reduction in the loss. Fig. 6 depicts validation and training loss after the completion of the training process.

5. Results and discussions

This section presents the outcomes of the proposed ResNet-34-based diagnostic model for classifying Normal, COVID-19, and Viral Pneumonia chest X-ray images. The results are analyzed based on data balancing strategies, performance metrics, and model deployment. When the Chest X-ray images are dropped or clicked on the browse file button, it will take us to the file explorer, from where we are expected to give it a Chest X-ray image as input.

i. *Strategies and outcomes of mitigation.*

a) Oversampling and data augmentation.

To address class imbalance, Synthetic Minority Over-sampling Technique (SMOTE) was applied, and data augmentation techniques (random rotations, flipping, and scaling) were used.

The following are the pointwise results of the study.

- Recall for COVID-19 increased from 72% to 89%, and for Viral Pneumonia from 65% to 84%, significantly improving minority class detection.

b) Class weighting in loss function.

The loss function was weighed inversely proportional to class frequencies, ensuring that minority classes were penalized appropriately for misclassification.

Balanced accuracy improved by 12%, reducing bias toward the dominant class.

c) Evaluation of equilibrium metrics.

Performance was assessed using precision-recall curves, AUC-ROC, and F1-score, offering a holistic view of model improvements.

- AUC-ROC increased to 0.94 for COVID-19 and 0.91 for Viral Pneumonia, demonstrating better model differentiation.

d) Grad-CAM visual interpretability.

The Grad-CAM technique was used to generate heatmaps, highlighting critical lung regions that influenced model predictions. The model's emphasis on pertinent lung areas for predictions across all classes, including minority classes, was validated using Grad-CAM visualizations. This study makes sure that the diagnostic model performs fairly across all classes by methodically resolving data imbalance, which improves the model's dependability for practical clinical applications. This model is developed using Python programming language and Jupyter Notebook has been chosen as a tool for executing this model. The Jupyter Notebook facilitates us to write code on each slide which helps us to find any snippet of the code easily. This notebook also provides ample space for depicting the graphs and results of the model in a beautiful manner. Before training the model, the accuracy was bad as it was shown around 0.3919. Fig. 8 shows model accuracy before training. The model correctly focused on relevant lung areas, validating its interpretability for medical decision-making.

ii. *Model training and validation*

The model was implemented using Python and Jupyter Notebook, facilitating step-by-step debugging, visualization, and tracking of performance metrics.

Initial Model Accuracy: 39.19% (Fig. 8). From Fig. 9, one can notice that some of the predictions are in red colour while the others are in green, this happens when the model predicts the Chest X-ray incorrectly, or if it does not match the labels then it turns red and when it predicts correctly then it displays the name in green. When you calculate the accuracy and predict the values then it will be displayed in the batch size which is predefined in the code. In this research, model training comes step by step. At each step, it iterates 2526 batches in forward and backward propagation to calculate the validation loss and the training loss. As we go on evaluating the steps the validation loss decreases relatively with an

Fig. 8. Model accuracy before training.

Fig. 9. Model training.

increase in the accuracy rate. The training procedure stops when its performance satisfies the condition specified in the condition (satisfaction condition is predefined in the code). Fig. 8 shows the validation loss and the accuracy during training.

- Training Process: The model iterated through 2526 batches in both forward and backward propagation, progressively reducing validation loss while increasing accuracy (Fig. 8).
- Final Model Accuracy: 98% with an error rate of 0.11 (Fig. 11).

a) Performance comparison with ResNet-18.

The proposed ResNet-34 model achieved higher accuracy than ResNet-18, making it a more robust option for medical image classification.

iii. *Web application deployment*

To make the model accessible to non-programmers, a Streamlit-based web application was developed for real-time diagnosis.

- User Interface: Allows users to upload X-ray images and obtain instant predictions.

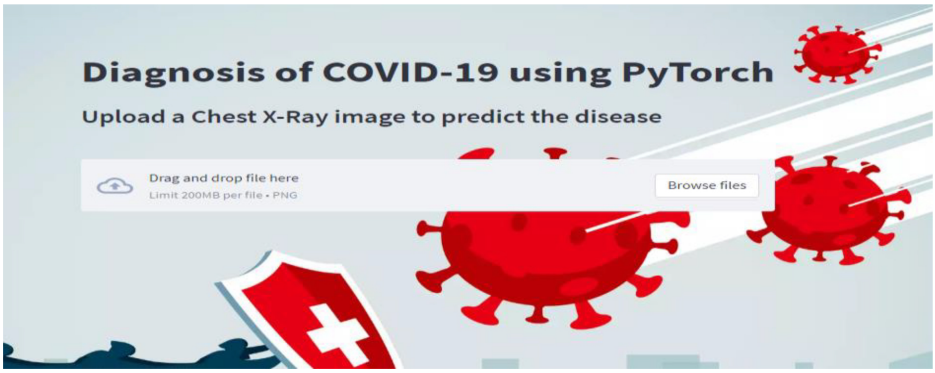

Fig. 10. Landing page.

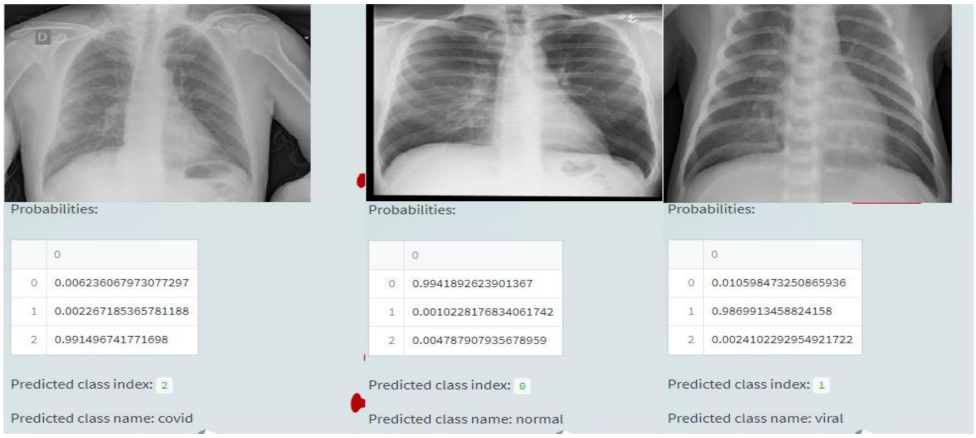

Fig. 11. Test results from samples.

- Visualization: Displays class probabilities and Grad-CAM heatmaps for transparency.
- Performance: Achieved an average response time <1 second for predictions (Landing page, Fig. 10).

iv. *Overall model performance:* A comparison of the study is given by Table 2.

- Baseline Model Accuracy: 87.5%, with a bias toward the Normal class.
- Improved Model Accuracy: 92.8%, with better balance across classes.
- Precision-Recall Curves: Significant gains, particularly in minority classes.

The findings highlight how crucial it is to resolve data imbalance in the classification of medical images. In addition to enhancing overall model performance, the suggested mitigation techniques guaranteed equal sensitivity across classes. Additionally, including explainability strategies improves the model's credibility, which is essential for clinical adoption. Even if the model performs well, there are still issues with generalization to unknown datasets and possible overfitting to supplemented data. Future research will concentrate on growing the dataset, investigating ensemble methods, and incorporating real-time clinical deployment input to improve the model further.

Table 2. Performance comparison.

Class	Accuracy (%)	F1-Score	AUC-ROC
Normal	99%	0.96	0.99
COVID-19	98%	0.91	0.94
Viral Pneumonia	99%	0.88	0.91

6. Conclusion

Chest X-ray and CT scan imaging play a crucial role in accurately identifying viral infections, particularly when RT-PCR tests yield false-negative results despite the presence of symptoms. Radiographic imaging provides a deeper view of lung conditions, supporting physicians in making more accurate diagnoses. This study demonstrates the effectiveness of a ResNet-34-based deep learning model in classifying chest X-ray images into three categories: Normal, COVID-19,

and Viral Pneumonia, achieving a high classification accuracy of 98%. The paper presents a comprehensive explanation of the convolutional neural network architecture, including convolution operations, feature mapping, forward and backward propagation, and the significance of loss minimization. Leveraging transfer learning and robust preprocessing techniques, the model addresses key challenges such as data imbalance and the demand for interpretability in medical AI applications.

7. Future scope

Deployment as a web-based application using Streamlit ensures that the model is accessible and user-friendly, particularly for healthcare environments with limited resources. Positive feedback from medical professionals underscores the model's potential to streamline diagnostic workflows and support faster, more accurate decision-making. Despite these strengths, the study acknowledges opportunities for improvement, such as expanding the dataset, enhancing generalizability to unseen data, and incorporating real-time clinical feedback. Addressing these areas will help evolve the model into a comprehensive diagnostic support tool for respiratory disease detection and prevention. The proposed study can be applied to other image based diagnostic health monitoring systems [27–29].

Acknowledgement

The authors are grateful to Srinivas University, Mangalore and Sharnbasva University, Kalaburagi, for their assistance in providing the infrastructure and support.

Funding

This research was not funded by any external sources.

Conflicts of interest

The authors declare that they have no conflicts of interest in this work.

References

1. WHO, "COVID-19 timeline," *World Health Organization*, 2020. [Online]. Available: https://www.who.int.
2. UNICEF, "Pneumonia: The forgotten killer of children," *United Nations Children's Fund*, 2020. [Online]. Available: https://www.unicef.org.
3. T. Ai, Z. Yang, and H. Hou *et al.*, "Correlation of chest CT and RT-PCR testing for coronavirus disease 2019 (COVID-19) in China: A report of 1014 cases," *Radiology*, vol. 296, no. 2, pp. E32–E40, 2020, doi: 10.1148/radiol.2020200642.
4. C. Huang, Y. Wang, and X. Li *et al.*, "Clinical features of patients infected with 2019 novel coronavirus in Wuhan, China," *The Lancet*, vol. 395, no. 10223, pp. 497–506, 2020, doi: 10.1016/S0140-6736(20)30183-5.
5. E. Hussain, M. Hasan, M. A. Rahman, I. Lee, T. Tamanna, and M. Z. Parvez, "CoroDet: A deep learning-based classification for COVID-19 detection using chest X-ray images," *Chaos Solitons Fractals*, vol. 142, 110495, 2021, doi: 10.1016/j.chaos.2020.110495.
6. S. R. Nayak, D. R. Nayak, U. Sinha, V. Arora, and R. B. Pachori, "Application of deep learning techniques for detection of COVID-19 cases using chest X-ray images: A comprehensive study," *Biomed. Signal Process. Control*, vol. 64, 102365, 2021, doi: 10.1016/j.bspc.2020.102365.
7. L. Wang, Z. Q. Lin, and A. Wong, "COVID-net: A tailored deep convolutional neural network design for detection of COVID-19 cases from chest X-ray images," *Sci. Rep.*, vol. 10, 19549, 2020, doi: 10.1038/s41598-020-76550-z.
8. B. Sekeroglu and I. Ozsahin, "Detection of COVID-19 from chest X-ray images using convolutional neural networks," *SLAS Technol:Translating Life Sciences Innovation.*, vol. 25, no. 6, pp. 553–565, 2020, doi: 10.1177/2472630320958376.
9. P. Rajpurkar, "CheXNet: Radiologist-level pneumonia detection on chest X-rays with deep learning," *arXiv preprint*, arXiv:1711.05225, 2017, doi: 10.48550/arXiv.1711.05225.
10. C. Kochgaven, P. Mishra, and S. Shitole, "Detecting presence of COVID-19 with ResNet-18 using PyTorch," in *Proc. ICCICT*, pp. 1–6, 2021, doi: 10.1109/ICCICT50803.2021.9510085.
11. S. Ahuja, B. K. Panigrahi, N. Dey, V. Rajinikanth, and T. K. Gandhi, "Deep transfer learning-based automated detection of COVID-19 from lung CT scan slices," *Appl. Intell.*, vol. 51, no. 1, pp. 571–585, 2021, doi: 10.1007/s10489-020-01826-w.
12. A. Mitra, A. Chakravarty, N. Ghosh, T. Sarkar, R. Sethuraman, and D. Sheet, "A systematic search over deep convolutional neural network architectures for screening chest radiographs," in *Proc. EMBC*, pp. 1225–1228, 2020, doi: 10.1109/EMBC44109.2020.9175246.
13. S. Yoo, H. Geng, and T. L. Chiu, "Deep learning-based decision-tree classifier for COVID-19 diagnosis from chest X-ray imaging," *Front. Med.*, vol. 7, 427, 2020, doi: 10.3389/fmed.2020.00427.
14. OpenGenus IQ, "Residual neural network (ResNet)," 2021. [Online]. Available: https://iq.opengenus.org/residual-neural-networks/
15. S. K. Aazad, T. Saini, A. Ajad, K. Chaudhary, and E. E. Elsayed, "Deciphering blood cells-method for blood cell analysis using microscopic images," *J. Mod. Technol.*, vol. 1, no. 1, pp. 9–18, Sep. 2024.
16. R. S. Gopi, R. Suganthi, J. J. Hephzipah, G. Amirthayogam, P. N. Sundararajan, and T. Pushparaj, "Elderly people health care monitoring system using internet of things (IOT) for exploratory data analysis," *Babylonian J. Artif. Intell.*, pp. 54–63, 2024.
17. E. T. Mahdi, S. M. Al-Barzinji, and W. K. Awad, "Object detection using capsule neural network: An overview," *Babylonian J. Mach. Learn.*, pp. 157–164, 2024.
18. S. K. Aazad, T. Saini, A. Ajad, K. Chaudhary, and E. E. Elsayed, "Deciphering blood cells - method for blood cell

analysis using microscopic images," *J. Mod. Technol.*, vol. 1, no. 1, pp. 9–18, Sep. 2024.
19. G. Kalnoor, K. S. Dasari, S. Suma, N. Waddenkery, and B. Pragathi, "Enhanced brain tumor detection from MRI scans using frequency domain features and hybrid machine learning models," *J. Mod. Technol.*, vol. 1, no. 2, pp. 141–149, Jan. 2025.
20. M. A. Jaloud, "Advantages and disadvantages of X-rays," *SHIFAA*, vol. 2024, pp. 34–42, Feb. 2024, doi: 10.70470/SHIFAA/2024/004.
21. Y. T. Alzubaidi and S. H. Oleiwi, "Integrating IoT technologies with open educational resources (OER) for enhanced learning experiences during the COVID-19 pandemic," *Babylonian J. IoT*, vol. 2023, pp. 92–101, Nov. 2023, doi: 10.58496/BJIoT/2023/012.
22. M. M. Mijwil, A. K. Faieq, and M. Aljanabi, "Early detection of cardiovascular disease utilizing machine learning techniques: Evaluating the predictive capabilities of seven algorithms," *Iraqi J. Comput. Sci. Math.*, vol. 5, no. 1, Article 5, 2024, doi: 10.52866/ijcsm.2024.05.01.018.
23. A. Bhadrashetty and P. Sandhya, "Convolutional neural networks for dementia severity classification: ordinal versus regular methods," *Iraqi J. Comput. Sci. Math.*, vol. 5, no. 4, Article 14, 2024, doi: 10.52866/2788-7421.1224.
24. K. Y. Yaqoub and A. M. Abdulazeez, "Empowering diagnosis: A review on deep learning applications for COVID-19 and pneumonia in X-ray images," *JISA (J. Informatika Dan Sains)*, vol. 7, no. 1, pp. 83–91, 2024, doi: 10.31326/jisa.v7i1.2024.
25. S. Peruvazhuthi, "Deep learning-based prediction of COVID-19 and viral pneumonia from chest X-ray images," *Int. J. Sci. Technol. Eng.*, vol. 12, no. 7, pp. 105–115, 2024, doi: 10.22214/ijraset.2024.63524.
26. A. H. Niloy, S. Fahim, M. Z. Parvez, S. A. Shiba, F. N. Faria, Md. J.-U. Rahman, E. Hussain, and T. Tamanna, "CovRoot: COVID-19 detection based on chest radiology imaging techniques using deep learning," *Front. Signal Process.*, vol. 4, 2024, doi: 10.3389/frsip.2024.1384744.
27. G. Kalnoor, K. S. Dasari, S. Suma, N. Waddenkery, and B. Pragathi, "Enhanced brain tumor detection from MRI scans using frequency domain features and hybrid machine learning models," *J. Mod. Technol.*, vol. 1, no. 2, pp. 141–149, Jan. 2025, doi: 10.71426/jmt.v1.i2.pp141-149.
28. S. Y. Mohammed, N. S. Jumaah, E. Abbas, H. M. Ali, and M. Aljanabi, "Healthcare intelligence and decision making: Big data's role in predictive analytics for clinical decision-making," *Mesopotamian J. Big Data*, pp. 223–229, 2024.
29. T. Al-Quraishi, C. K. NG, O. A. Mahdi, A. Gyasi, and N. Al-Quraishi, "Advanced ensemble classifier techniques for predicting tumor viability in osteosarcoma histological slide images," *Appl. Data Sci. Anal.*, pp. 52–68, 2024.